nature biotechnology

In vivo delivery of siRNA to immune cells by conjugation to a TLR9 agonist enhances antitumor immune responses

Marcin Kortylewski[1], Piotr Swiderski[2], Andreas Herrmann[1], Lin Wang[1], Claudia Kowolik[2], Maciej Kujawski[1], Heehyoung Lee[1], Anna Scuto[2], Yong Liu[1], Chunmei Yang[1], Jiehui Deng[1], Harris S Soifer[3], Andrew Raubitschek[1], Stephen Forman[4], John J Rossi[3], Drew M Pardoll[5], Richard Jove[2] & Hua Yu[1]

© 2009 Nature America, Inc. All rights reserved.

Efficient delivery of small interfering (si)RNA to specific cell populations *in vivo* remains a formidable challenge to its successful therapeutic application. We show that siRNA synthetically linked to a CpG oligonucleotide agonist of toll-like receptor (TLR)9 targets and silences genes in TLR9$^+$ myeloid cells and B cells, both of which are key components of the tumor microenvironment. When a CpG-conjugated siRNA that targets the immune suppressor gene *Stat3* is injected in mice either locally at the tumor site or intravenously, it enters tumor-associated dendritic cells, macrophages and B cells. Silencing of *Stat3* leads to activation of tumor-associated immune cells and ultimately to potent antitumor immune responses. Our findings demonstrate the potential of TLR agonist–siRNA conjugates for targeted gene silencing coupled with TLR stimulation and immune activation in the tumor microenvironment.

The ability of siRNAs to control the expression of specific genes makes them an attractive new class of drugs with broad potential for the treatment of diverse human diseases. Several recent studies have shown the feasibility of *in vivo* siRNA delivery, demonstrating therapeutic efficacy in mouse models[1–4] and nonhuman primates[5,6]. Nevertheless, efficient targeting of siRNA to specific cell types that are important constituents of the tumor microenvironment and active players in promoting tumor progression remains challenging.

The immune system can serve as an extrinsic tumor suppressor[7–9]. However, the tumor microenvironment is characterized by a lack of tumor-specific CD8$^+$ T cells and an excess of regulatory T cells and myeloid-derived suppressor cells that promote tumor immune evasion[10,11]. Myeloid cells and other immune cells in the tumor microenvironment also produce growth factors and angiogenic/metastatic factors critical for tumor progression[12]. The orchestration of these processes in the tumor microenvironment appears to be highly dependent on the oncogenic transcription factor Stat3 (refs. 13–17). In particular, we and others have recently demonstrated a role for Stat3 in mediating tumor immune evasion[10,17,18]. Activated Stat3 in myeloid cells inhibits expression of a large number of immunostimulatory molecules related to T-helper cell 1 (Th1)-type responses while promoting production of several key immunosuppressive factors[17,19,20] as well as angiogenic factors[12]. In addition, by mediating signaling of certain cytokines and growth factors, notably interleukin (IL)-6, Stat3 activation in myeloid cells activates Stat3 in tumor cells, enhancing tumor cell proliferation and survival[21–24]. Because Stat3 also restrains TLR-mediated Th1 immune responses[10,17,25], we reasoned that simultaneously silencing *Stat3* by siRNA and activating TLRs by their agonists could effectively shift the tumor microenvironment from pro-oncogenic to antitumor. A recent study using polymer-mediated *in vivo* transfection of 5′-triphosphate-*Bcl2* siRNA has demonstrated the benefits of simultaneously inducing antitumor immunity and silencing a pro-oncogenic gene[4].

Here we explored a strategy of linking siRNAs to synthetic oligonucleotide agonists of endosomal TLRs to combine targeted delivery to immune cells with TLR-dependent activation of antitumor immune responses. The endosomal location of oligonucleotide-binding TLRs such as TLR3, TLR7, TLR8 and TLR9 (refs. 26–28) might be advantageous in facilitating the uptake of the siRNA component into the cytosol for efficient gene silencing. To validate this concept, we chose TLR9-specific oligodeoxynucleotides containing an unmethylated CpG motif (CpG oligonucleotide), which are already in clinical trials for melanoma[29]. Additionally, CpG oligonucleotides are efficiently internalized by various antigen-presenting cells, such as dendritic cells (DCs), macrophages and B cells. Their binding to TLR9 can initiate a cascade of innate and adaptive immune responses[28–30]. Myeloid cells and B cells are critical components of the tumor microenvironment that actively promote oncogenesis[12,17,19,21,22]. By linking the single-stranded CpG oligonucleotide with double-stranded siRNA, we have created a single synthetic molecule capable of delivering siRNA to myeloid and B cells, of silencing an immune checkpoint and oncogenic gene and of activating TLRs, leading to therapeutic antitumor immune responses.

[1]Departments of Cancer Immunotherapeutics & Tumor Immunology, [2]Molecular Medicine, [3]Molecular Biology and [4]Hematopoietic Cell Transplant, Beckman Research Institute at City of Hope, Duarte, California, USA. [5]Sidney Kimmel Cancer Center, Johns Hopkins University School of Medicine, Baltimore, Maryland, USA. Correspondence should be addressed to H.Y. (hyu@coh.org).

Received 23 April; accepted 25 August; published online 13 September 2009; doi:10.1038/nbt.1564

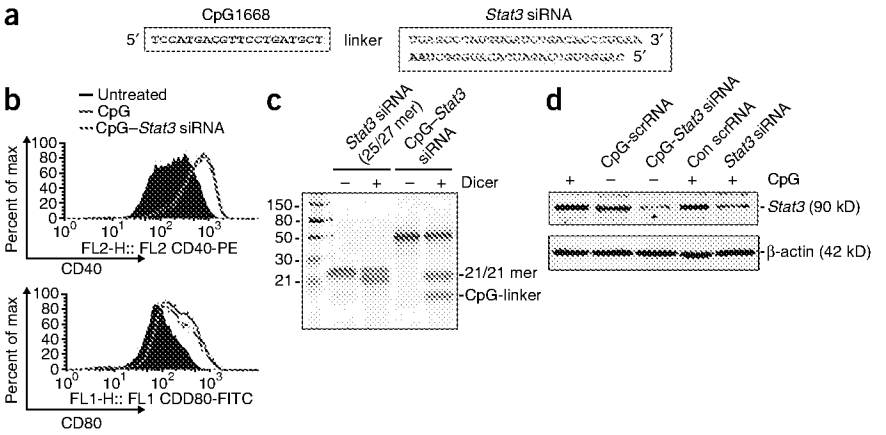

Figure 1 Structure and function of the CpG–*Stat3* siRNA conjugate. (**a**) Sequence of the CpG-linked mouse *Stat3* siRNA conjugate (CpG1668-*Stat3* siRNA): CpG1668 sequence (deoxyribonucleotides shown in black) were phosphothioated and connected through a carbon linker (6 of C3 units) to the antisense strand of *Stat3* siRNA (ribonucleotides shown in red). (**b**) CpG-siRNA has similar immunostimulatory activity compared to uncoupled CpG oligonucleotides, as indicated by increased expression of costimulatory molecules, CD40 and CD80, on primary splenic DCs after 24 h incubation with or without oligonucleotides; splenocytes were pooled from two to three mice and the experiment was performed twice with similar results. (**c**) Linked CpG–*Stat3* siRNA is processed to active 21-mer siRNA by recombinant Dicer *in vitro*. Processing of conjugated CpG–*Stat3* siRNA molecules and *Stat3* siRNA were visualized on polyacrylamide gel through SYBR Gold staining; position of the 21/21mer and the remaining part of the molecule (CpG plus carbon linker) are indicated. Full-length gel is presented in **Supplementary Figure 13a**. (**d**) *Stat3* siRNA linked to CpG oligonucleotide retains the ability to mediate RNA interference. B16 cells were transfected, using Lipofectamine, with CpG-linked double-stranded (ds)RNAs or unconjugated dsRNAs plus 15 nM CpG oligonucleotide. *Stat3* gene-silencing effects were evaluated by western blot analysis. Full-length blots are presented in **Supplementary Figure 13b**.

© 2009 Nature America, Inc. All rights reserved.

RESULTS

Construction of the CpG–*Stat3* siRNA conjugate molecule

The antisense strand of the siRNA (27 mer) was coupled to a TLR9 agonist, CpG1668 oligonucleotide[31,32] using a carbon chain linker and hybridized to the 25-mer sense strand of the siRNA as shown in **Figure 1a**. A 25/27mer siRNA was chosen over the conventional 21-mer duplex to allow uncoupling of the siRNA from the CpG sequence by the Dicer enzyme once inside the cell. The asymmetric 25/27mer siRNA was optimized for specific processing by Dicer and was more potent in target gene silencing[33,34]. Adding either CpG1688 alone or CpG–*Stat3* siRNA conjugate to cultured DC2.4 dendritic cells resulted in a similar increase in expression of costimulatory CD40 and CD80 molecules, suggesting that CpG–*Stat3* siRNA conjugate retains its capacity to activate TLR9 (**Fig. 1b**). In addition, the immunostimulatory properties of CpG-siRNA conjugates do not differ from the effect of CpG alone as measured by production of inflammatory cytokines in primary cells and NF-κB/AP1 activation in a stable macrophage cell line (**Supplementary Fig. 1**). To assess whether linking siRNA with CpG moiety would still allow Dicer processing, we compared *in vitro* Dicer activity on CpG–*Stat3* siRNA substrate versus 25/27mer *Stat3* siRNA. Both the CpG–*Stat3* siRNA and *Stat3* siRNA were processed to 21mer siRNA by recombinant Dicer (**Fig. 1c**). Finally, to determine whether the CpG–*Stat3* siRNA retains gene silencing function, the chimeric molecule was transfected into cells using Lipofectamine. Linking CpG oligonucleotide to siRNA did not interfere with *Stat3* gene silencing (55% and 49% at protein level, respectively, as measured by densitometry) (**Fig. 1d**).

In vitro uptake and gene silencing effects of the CpG-siRNA

To determine the specificity and efficiency of CpG-siRNA uptake, we incubated freshly prepared mouse splenocytes with CpG-*Stat3* siRNA or an unconjugated *Stat3* siRNA, in the absence of transfection reagents. Both the CpG–*Stat3* siRNA and unconjugated *Stat3* siRNA were labeled with fluorescein isothiocyanate (FITC). Fluorescein labeling of DCs, macrophages, B cells, granulocytes and T cells was assessed by flow cytometry, which indicated that the chimeric CpG–*Stat3* siRNA was efficiently taken up by both plasmacytoid ($CD11c^+B220^+$) and conventional ($CD11c^+B220^-$) splenic DCs, macrophages ($F4/80^+Gr1^-$) and B cells ($B220^+CD11c^-$), but only minimally by splenic granulocytes ($Gr1^+F4/80^-$) or T cells ($CD3^+$) (**Fig. 2a**, **Supplementary Fig. 2** and **Supplementary Table 1**). This uptake pattern reflects the known distribution of TLR9 expression in murine leukocyte subsets[26,35]. Analysis of intracellular staining of TLR9 in fixed $CD11c^+$ DCs by flow cytometry confirmed TLR9 expression (**Fig. 2a**, bottom right). Unconjugated *Stat3* siRNA was not efficiently incorporated into DCs even after 24 h incubation, demonstrating that linkage to the TLR9 ligand facilitates siRNA uptake (**Fig. 2a**, bottom left).

We further evaluated CpG–*Stat3* siRNA–FITC uptake by DC 2.4 mouse DCs. Flow cytometry and fluorescent microscopy indicated that CpG–*Stat3* siRNA–FITC was internalized by DC 2.4 cells with kinetics similar to CpG-oligonucleotides alone (**Fig. 2b**, two top rows; and **Supplementary Fig. 3**) and to those reported previously[36]. By 60 min, >80% of the DC 2.4 cells were positive for uptake of the conjugate, which was confirmed by confocal microscopic analysis. The uptake of the CpG–*Stat3* siRNA–FITC was dose dependent (**Fig. 2b**, bottom row).

Confocal microscopic analyses further showed that at 1 h after incubation, the CpG–*Stat3* siRNA colocalized with TLR9 within perinuclear endocytic vesicles (**Fig. 2c**, two top rows; and **Supplementary Fig. 4**). This colocalization diminished at 2 and 4 h after CpG–*Stat3* siRNA treatment (**Fig. 2c**, two top rows). Previous studies have demonstrated that binding of the Dicer nuclease to the siRNA oligonucleotide is required for further siRNA processing to shorter 21-mer fragments that mediate RNA-induced silencing complex–dependent mRNA degradation[37]. We observed transient colocalization of the CpG–*Stat3* siRNA with Dicer within 2 h after adding the oligonucleotide to cultured DCs (**Fig. 2c**, two bottom rows; and **Supplementary Fig. 4**). The colocalization of CpG–*Stat3* siRNA and Dicer became weaker by 4 h (**Fig. 2c**) and undetectable after 24 h (data not shown).

Gene silencing effects of the CpG–*Stat3* siRNA in DC2.4 cells were determined by quantitative real-time PCR analysis of the *Stat3* mRNA (**Fig. 2d**). Maximum effect on *Stat3* silencing was observed at a relatively high concentration of CpG–*Stat3* siRNA (1 μM) in serum-containing cell culture medium. GpC-conjugated *Stat3* siRNA, which binds but does not activate TLR9 (ref. 36), failed to silence *Stat3*, suggesting a possible requirement of TLR9 activation for the CpG-siRNA to be processed. Further experiments demonstrated that in *TLR9*$^{-/-}$ myeloid cells and DCs, cellular uptake of CpG–*Stat3* siRNA

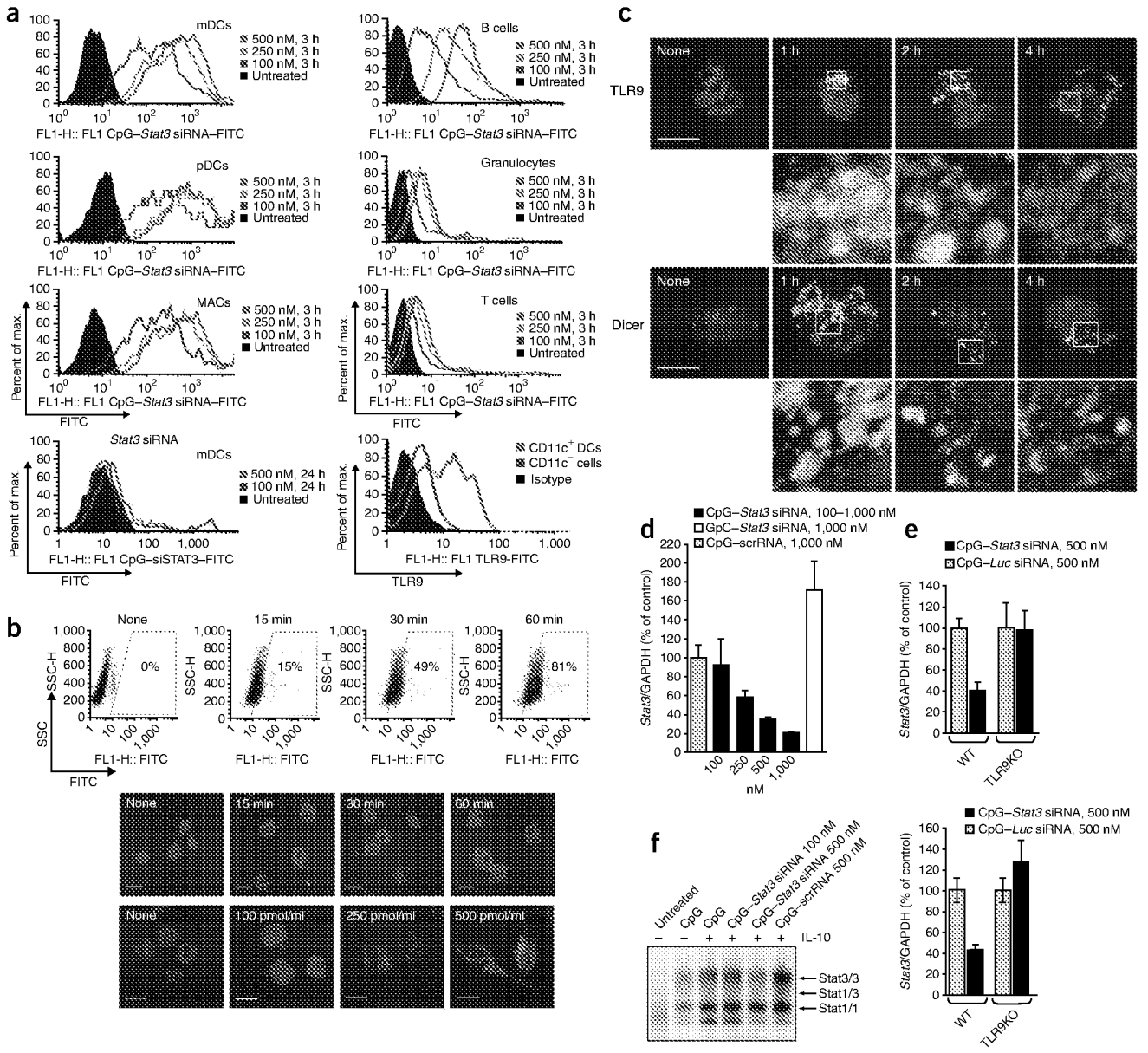

Figure 2 Uptake and gene silencing by CpG–*Stat3* siRNA *in vitro*. (**a**) Targeted delivery: splenocytes were incubated for 3 h with CpG–*Stat3* siRNA or for 24 h with unconjugated *Stat3* siRNA labeled with FITC (bottom left panel), without any transfection reagents. Percentage of FITC-positive $CD11c^+B220^-$ nonplasmacytoid (mDCs) and $CD11c^+B220^+$ plasmacytoid (pDCs) DCs, $F4/80^+Gr1^-$ macrophages (MACs), $B220^+CD11c^-$ B cells, $Gr1^+F4/80^-$ granulocytes and $CD3^+$ T cells was assessed by flow cytometric analysis (**Supplementary Table 1**). Splenic $CD11c^+$ DCs express high levels of TLR9. Intracellular staining of TLR9 as shown in fixed splenic DCs by flow cytometry (bottom right). Similar results were obtained in two independent experiments. (**b**) Kinetics of CpG-siRNA internalization. CpG–*Stat3* siRNA–FITC is quickly internalized by DCs without transfection reagents. The uptake by DC2.4 cells is analyzed by flow cytometry (top row) and confocal microscopy (two lower rows) after incubation with CpG–*Stat3* siRNA–FITC (500 nM) for indicated times (two upper rows) or after 1 h incubation at indicated concentrations (bottom row); results are representative of three independent experiments. SSC, side scatter. Scale bar, 10 μm. (**c**) Internalized CpG–*Stat3* siRNA colocalizes with TLR9 (two upper rows) and transiently interacts with Dicer (two lower rows). DC2.4 cells were incubated with 500 nM of CpG–*Stat3* siRNA for indicated times. Shown are confocal microscopy images; green, CpG–*Stat3* siRNA–FITC; red, immunofluorescent detection of endogenous TLR9 or Dicer; blue, nuclear staining with DAPI. Scale bar, 10 μm. All confocal imaging studies were performed at least three times with similar results and the images acquired were characteristic for the majority of analyzed cells (**Supplementary Fig. 4**). (**d**) Dose-dependent gene-silencing effects of CpG–*Stat3* siRNA, compared to GpC-*Stat3* siRNA at the highest dose, as determined by quantitative real-time PCR in DC2.4 cells. Shown are the results of real-time PCR for *Stat3*, normalized to *GAPDH* expression levels. The level of *Stat3* expression in CpG–scrambled RNA sample is set at 100%. Shown are means ± s.e.m. from three independent experiments analyzed in duplicate. (**e**) *Stat3* silencing is impaired in *TLR9*-deficient primary myeloid cells (top) and DCs (bottom). Shown are the results of two independent experiments, analyzed in triplicate by real-time PCR; means ± s.e.m. (**f**) Stat3 DNA-binding is reduced after 48 h incubation of CpG–*Stat3* siRNA, relative to CpG–scrambled RNA, in DC2.4 cells. Shown are results of electrophoretic mobility gel-shift assay using radiolabeled probe specifically bound by Stat3 and Stat1, data representing three independent experiments. Positions of Stat dimers are indicated. Full-length gel is presented in **Supplementary Figure 13c.**

© 2009 Nature America, Inc. All rights reserved.

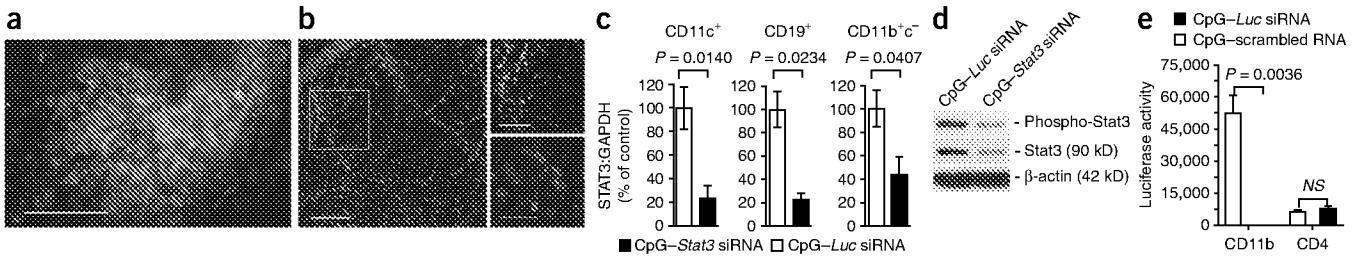

Figure 3 Treatment with CpG–*Stat3* siRNA leads to cell-specific gene silencing *in vivo*. (**a**) *In vivo* uptake by myeloid cells of peritumorally injected CpG–*Stat3* siRNA. Shown is immunofluorescent staining of frozen tumor tissue section 6 h after injection of CpG-siRNA conjugate. Green, FITC-labeled CpG–*Stat3* siRNA; red, myeloid cells stained with anti-CD11b antibodies; blue, nuclear staining with Hoechst. Scale bar, 50 μm. (**b**) Left panel: intravital two-photon microscopy imaging on TDLN at 1 h after peritumoral injection of FITC-labeled CpG–*Stat3* siRNA (green); blood vessels stained with dextran-rhodamine (red); Hoechst-stained nuclei (blue). Scale bar, 200 μm. Top right panel: close-up of the lymph node tissue to visualize FITC-positive cells entering the lymph node; scale bar = 100 μm. Bottom right panel: intracellular distribution of FITC-labeled CpG–*Stat3* siRNA. Scale bar, 25 μm. Results represent two independent experiments. (**c**,**d**) Repeated local peritumoral treatment with CpG–*Stat3* siRNA significantly reduces *Stat3* mRNA and protein in immune cells within TDLNs. Total RNA and protein were isolated from CD11c$^+$ DCs, CD19$^+$ B cells and CD11b$^+$c$^-$ myeloid cells accumulated in TDLNs (inguinal) using cells pooled from four to nine mice. (**c**) Shown are quantitative real-time PCR results on *Stat3* expression, combining three to four independent experiments ± s.e.m.; control CpG-*Luc* siRNA was set at 100%. (**d**) Total and phospho-Stat3 levels are reduced by CpG–*Stat3* siRNA conjugates. Representative results of western blot analysis for tyrosine-phosphorylated or total Stat3 and β-actin from one of two independent experiments are shown. Full-length blots are presented in **Supplementary Figure 13d**. (**e**) Two weeks after B16 tumor challenge, luciferase-overexpressing mice were injected peritumorally with CpG–*Luc* siRNA or CpG–scrambled RNA every day for 3 d. The level of luciferase activity was assessed in CD11b$^+$ and CD4$^+$ cells isolated from TDLNs; shown are representative results from one of three independent experiments using three mice/group/experiment. NS, not significant.

© 2009 Nature America, Inc. All rights reserved.

was normal (**Supplementary Fig. 5**), but the gene silencing effect of CpG–*Stat3* siRNA was impaired (**Fig. 2e**). We also confirmed the gene silencing effects using electrophoretic mobility shift assays (EMSA) to detect Stat3 DNA-binding activity in DC2.4 cells, which was induced by IL-10 stimulation (**Fig. 2f**). Note that, as indicated above, stimulation using CpG itself also resulted in Stat3 activation[25,38] (**Fig. 2f**), thereby complicating the EMSA analysis for detection of *Stat3* silencing. Nonetheless, at higher concentrations, CpG–*Stat3* siRNA diminished Stat3 DNA-binding activity relative to the conjugate scrambled RNA controls. To demonstrate the generality of this approach to gene silencing, we used TLR9-positive mouse A20 B-cell lymphoma cells to test CpG-siRNA internalization (**Supplementary Fig. 6a**) and gene silencing. A chimeric conjugate linking the CpG1668 oligonucleotide with an siRNA specific for firefly luciferase efficiently reduced luciferase activity in A20-Luc cells (**Supplementary Fig. 6b**).

The CpG–*Stat3* siRNA conjugate *in vivo*

Biodistribution experiments in naive tumor-free mice confirmed that CpG–*Stat3* siRNA is specifically internalized by resident macrophages in different tissues as well as DCs and B cells in lymph nodes (**Supplementary Fig. 7**). We next assessed the uptake of the CpG–*Stat3* siRNA by macrophages and DCs in tumor-bearing mice. C57BL/6 mice with B16 tumors were injected peritumorally with CpG–*Stat3* siRNA–FITC at 0.78 nmol (20 μg)/injection. Immunofluorescent staining showed myeloid cells positive for CpG–*Stat3* siRNA accumulated at the injection site (**Fig. 3a**). Flow cytometry also indicated the presence of CpG–*Stat3* siRNA in tumor-associated myeloid cells (**Supplementary Fig. 8a**). Furthermore, *in vivo* intravital two-photon microscopy showed the presence of FITC-positive cells in tumor-draining lymph node (TDLN), as early as 1 h after injection of the labeled construct (**Fig. 3b**, **Supplementary Fig. 8b** and **Supplementary Fig. 9**), but not in the contralateral lymph nodes (**Supplementary Fig. 9**). Additionally, high-resolution imaging by intravital two-photon microscopy revealed an increased number of FITC-positive cells in TDLNs, as well as an accumulation of FITC-labeled CpG–*Stat3* siRNAs in perinuclear endocytic vesicles (**Fig. 3b**, bottom right), which was also observed in cultured DCs (**Fig. 2c**).

We next evaluated the gene silencing and antitumor effects of CpG–*Stat3* siRNAs *in vivo*. Peritumoral injections of the CpG–*Stat3* siRNA resulted in effective gene silencing in DCs, macrophages and B cells in TDLNs, compared to control CpG-*Luc* siRNA, as measured by quantitative real-time PCR (**Fig. 3c**). Stat3 inhibition in CD11c$^+$ DCs isolated from TDLNs was confirmed at protein level (**Fig. 3d**). Furthermore, quantitative real-time PCR and western blot analysis indicated *Stat3* silencing in the total TDLNs (**Supplementary Fig. 10**). We also used CpG-*Luc* siRNA conjugate to confirm that CpG-siRNA conjugates are able to reduce protein expression specifically within myeloid cells *in vivo*. Mice overexpressing firefly luciferase under control of the β-actin promoter[39] were challenged with tumor cells, followed by repeated peritumoral injections of CpG-*Luc* siRNA. Results from these experiments indicated effective inhibition of luciferase activity in CD11b$^+$ myeloid cells but not in CD4$^+$ lymphocytes within TDLNs (**Fig. 3e**).

Both DCs and macrophages in the tumor microenvironment are known to promote immune tolerance[11,17]. Our previous work demonstrated that Stat3 is persistently activated in myeloid cells in the tumor milieu and that genetic ablation of *Stat3* in the myeloid compartment elicits potent antitumor immunity[10]. Furthermore, both CpG and lipopolysaccharide treatment activates Stat3 (refs. 25,38,40), which acts as a negative feedback mechanism to constrain Th1 immune responses. Therefore, we assessed whether the CpG–*Stat3* siRNA conjugates could reverse the immunosuppressive effects imposed by the tumor microenvironment and at the same time allow effective antitumor immunity induced by TLR9 triggering. Local treatment with CpG–*Stat3* siRNA oligonucleotides inhibited growth of subcutaneously growing B16 melanoma (3–5 mm in diameter at the initial treatment). In contrast, treatment with unconjugated CpG oligonucleotide plus *Stat3* siRNA, or CpG–scrambled RNA construct, or GpC-*Stat3* siRNA had only minor antitumor effects (**Fig. 4a**). The antitumor effects of CpG–*Stat3* siRNA were confirmed by using two alternative *Stat3* siRNA sequences (data not shown). To directly show that the antitumor effects induced by CpG–*Stat3* siRNA were mainly mediated by immune cells, we performed *in vivo* experiments with antibody-mediated depletion of CD8$^+$/CD4$^+$ T cells and natural killer (NK) cells. Without CD8$^+$ and CD4$^+$ immune cell populations (possibly also the cross-priming

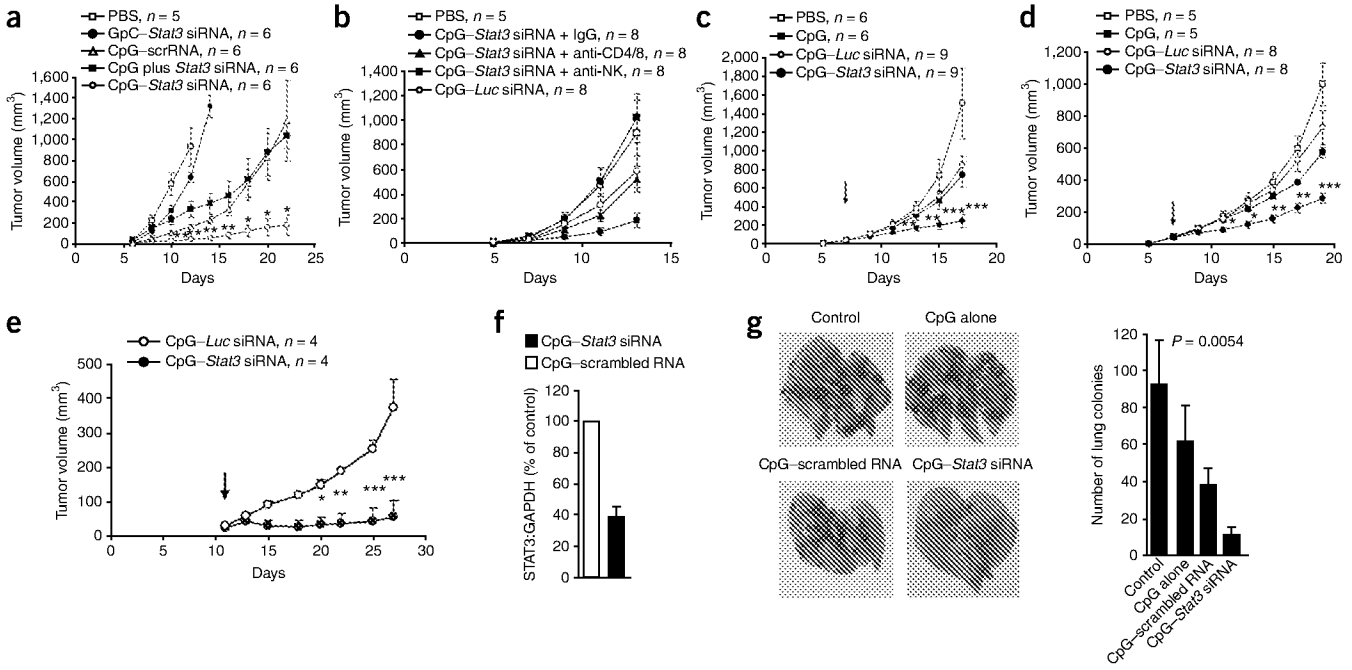

Figure 4 Both local and systemic treatments with CpG–*Stat3* siRNA inhibit tumor growth. (**a**) Mice with subcutaneous (s.c.) B16 tumors were treated by peritumoral injections of CpG–*Stat3* siRNA, GpC-*Stat3* siRNA, CpG–scrambled RNA, combination of equimolar amounts of uncoupled CpG and *Stat3* siRNA (CpG plus *Stat3* siRNA) or PBS only every other day, starting 6 d after challenge with 1×10^5 B16 cells, $n = 5$–6. Statistically significant differences between CpG–*Stat3* siRNA– and CpG–scrambled RNA–treated groups are indicated by asterisks. ***; $P < 0.001$; **, $P < 0.01$; *, $P < 0.05$. Similar results were obtained in three independent experiments. (**b**) Tumor growth inhibition by CpG–*Stat3* siRNA involves NK cell– and T cell–mediated immunity. Mice with established B16 tumors were depleted of NK cell or $CD4^+/CD8^+$ lymphocytes before CpG–*Stat3* siRNA treatment; shown are means ± s.e.m. $P < 0.0001$ (from two-way ANOVA test). (**c**,**d**) Local treatment with CpG–*Stat3* siRNA reduces growth of C4 melanoma (**c**) and CT26 colon carcinoma (**d**). Tumor cells were injected subcutaneously into C3H or BALB/c mice, respectively. Mice with established tumors were treated by peritumoral injections of CpG–*Stat3* siRNA, CpG–*Luc* siRNA, CpG alone or PBS every other day, starting 7d after challenge with 1×10^5 tumor cells. Statistically significant differences between the CpG-siRNA–treated groups are indicated by asterisks. ***, $P < 0.001$; **, $P < 0.01$; *, $P < 0.05$. (**e**) C57BL/6.CEA mice were challenged subcutaneously with 1×10^5 of MC38.CEA cells and treated as described above using CpG–*Stat3* siRNA or CpG–*Luc* siRNA starting from day 11 after tumor challenge. $P < 0.0001$ by two-way ANOVA ($n = 4$ for each group). ***, $P < 0.001$; **, $P < 0.01$; *, $P < 0.05$. (**f**) Systemic treatment with CpG–*Stat3* siRNA reduces *Stat3* expression in DCs within TDLNs (cervical). Samples pooled from six mice/group were analyzed by real-time PCR. Shown is the average level of *Stat3* expression in CpG–*Stat3* siRNA–treated mice from one of two independent experiments analyzed in triplicates ± s.e.m., relative to control CpG–scrambled RNA, which was set as 100%. (**g**) Systemic treatment with CpG–*Stat3* siRNA reduces the number of B16 tumor metastasis. Mice were intravenously injected with B16 cells and treated with CpG alone, CpG–*Stat3* siRNA or CpG–scrambled RNA i.v. injections every other day starting from 2 d after tumor challenge. Lung colonies were enumerated 15 d later when control mice became moribund. Shown are mean numbers of colonies ± s.e.m. ($n = 7$). $P = 0.0054$ by two-way ANOVA test. Representative photos of lung tissues excised from mice inoculated and treated as described above. The *in vivo* data are representative of two independent experiments.

© 2009 Nature America, Inc. All rights reserved.

$CD11c^+CD8^+$ DCs), the effects of CpG–*Stat3* siRNA treatment were reduced (**Fig. 4b**). The therapeutic effects of CpG–*Stat3* siRNA were abrogated in the absence of NK cells (**Fig. 4b**).

We confirmed that local treatment with CpG–*Stat3* siRNA can reduce growth of other tumors independently of their genetic background. CpG–*Stat3* siRNA oligonucleotides inhibited growth of both a poorly immunogenic variant of K1735 melanoma, C4 (ref. 41), and CT26 colon carcinomas in C3H and BALB/c mice, respectively (**Fig. 4c**,**d**). Furthermore, CpG–*Stat3* siRNA treatment of the carcinoembryonic antigen (CEA) transgenic C57BL/6 mice bearing MC38 colon carcinomas expressing CEA led to tumor regression in three out of four mice (**Fig. 4e**). To assess *in vivo* effects of the CpG–*Stat3* siRNA on tumor cells, we stained B16 tumor tissues with fluorescent antibody specific to activated caspase-3. B16 tumors treated with CpG–*Stat3* siRNA had undergone more extensive apoptosis than the tumors in the other three treatment groups (**Supplementary Fig. 11**). We also investigated the possibility that CpG–*Stat3* siRNA could be systemically delivered to achieve gene silencing and antitumor effects. Intravenous injection (i.v.) of CpG–*Stat3* siRNA (0.78 nmol) reduced *Stat3* expression in DCs within TDLNs relative to CpG–scrambled RNA (**Fig. 4f**). Systemic delivery of CpG–*Stat3* siRNA to inhibit metastasis was tested in an experimental B16 lung metastasis model. Relatively small amounts of the oligonucleotide (<1 mg/kg) were used for the systemic injection, which led to significant reduction in the number of lung metastases ($P = 0.0054$; **Fig. 4g**). Lower antitumor effect was also observed with CpG–scrambled RNA and CpG oligonucleotide alone. Thus, maximal antitumor effects required conjugation of the CpG TLR9 ligand with a functional *Stat3* siRNA.

Modulation of the tumor milieu by the CpG–*Stat3* siRNA

To further assess the role of immune modulation in the observed antitumor effects mediated by CpG–*Stat3* siRNA conjugate treatment, we analyzed changes in Th1 cytokine and/or chemokines and costimulatory molecule expression by DCs in the TDLNs. Lack of *Stat3* in DCs has been shown to upregulate expression of Th1 cytokines/chemokines[10,20,42,43], which can be greatly amplified by CpG treatment[25]. Injection of the CpG–*Stat3* siRNA at the tumor site resulted in upregulation of several Th1 cytokines and chemokines, which were known to be upregulated by *Stat3* ablation[10,20,42,43] (**Fig. 5a**). It has also been documented that

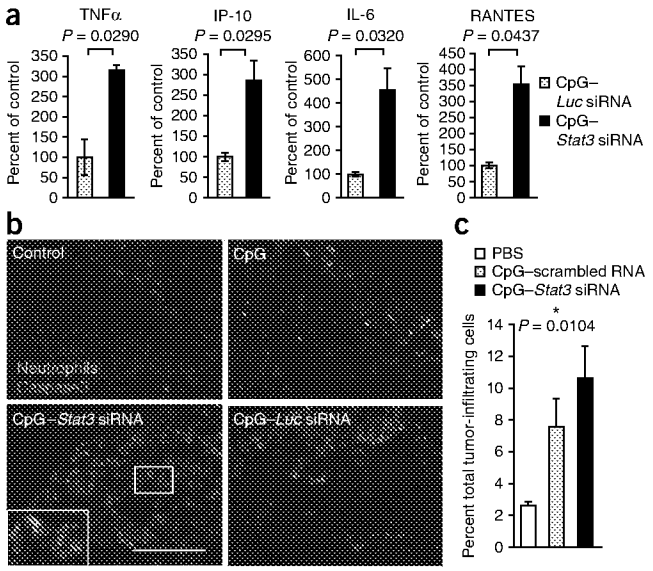

Figure 5 *In vivo* administration of CpG–*Stat3* siRNA induces innate immunity. (**a**) Immunostimulatory cytokine and/or chemokine gene expression was analyzed in DCs enriched from TDLN cell suspensions pooled from four to ten mice, prepared after three peritumoral injections of CpG–*Stat3* siRNA or CpG-*Luc* siRNA. Data from quantitative real-time PCRs run in triplicates were normalized to *GAPDH* expression. The averaged results from four independent *in vivo* experiments were combined and analyzed for statistical significance using an unpaired *t*-test with unequal variance. Shown are mean values ± s.e.m.; CpG–*Luc* siRNA was set as a baseline (100%). (**b**) Frozen sections of tumor tissues isolated from mice after indicated treatments were stained with antibodies specific to neutrophils (green) and activated caspase-3 (red) and analyzed by fluorescent microscopy. Shown are results representative of two independent experiments. Scale bar, 200 μm. (**c**) Single-cell suspensions prepared from tumors pooled from three to six mice were analyzed by flow cytometry for the presence of Gr1$^+$CD11b$^-$ neutrophils. Shown are means ± s.e.m. combined from three independent experiments.

DCs with low expression levels of costimulatory molecules mediate immune tolerance[44], which is one of the proposed mechanisms for tumor-immune evasion induced by Stat3 activation in tumor-associated DCs[10]. We therefore analyzed expression of costimulatory molecules by DCs enriched from TDLNs. CpG–*Stat3* siRNA treatment reduced the number of the DCs with low expression of costimulatory molecules, including major histocompatibility complex (MHC) class II, CD80 and CD40, which was accompanied by a modest increase in expression of these costimulatory molecules (**Supplementary Fig. 12**). *Stat3* ablation in myeloid cells followed by local treatment using CpG oligonucleotide has been shown to induce potent antitumor innate immune responses that involve neutrophils[25]. We therefore assessed whether CpG–*Stat3* siRNA conjugate treatment could lead to neutrophil-associated tumor cell apoptosis. Costaining B16 tumor tissue sections with antibodies specific to activated caspase-3 and neutrophils revealed that CpG–*Stat3* siRNA treatment induced massive tumor cell apoptosis (activated caspase-3 positive), which was associated with an increase in tumor-infiltrating neutrophils (**Fig. 5b**). The increased number of neutrophils in the tumor after CpG–*Stat3* siRNA, and to slightly lesser extent after CpG–*Luc* siRNA, treatment was further confirmed by flow cytometry (**Fig. 5c**).

The ratio of effector to regulatory T cells within the tumor microenvironment is considered indicative of the effect of adaptive immune responses on tumor progression and metastasis[45]. We investigated the numbers of tumor-infiltrating T-cell populations in subcutaneously growing B16 tumors treated locally for 2 weeks with CpG–*Stat3* siRNA, CpG–scrambled RNA control or PBS only. Although CpG–*Stat3* siRNA treatment did not induce significant changes in overall CD4$^+$ T-cell numbers within the tumors, as shown by flow cytometric analysis (**Fig. 6a**), the percentage of CD4$^+$/FoxP3$^+$ Treg cells within all CD4$^+$ T cells dropped from ~60% to 25% after peritumoral injections of CpG–*Stat3* siRNA (**Fig. 6b**). We observed an increase in the infiltration of total CD8$^+$ T cells in the tumor stroma, although CpG–scrambled RNA control treatment also led to some recruitment of CD8$^+$ T cells (**Fig. 6c**). These effects probably result from TLR9-mediated immunostimulation of tumor-infiltrating

© 2009 Nature America, Inc. All rights reserved.

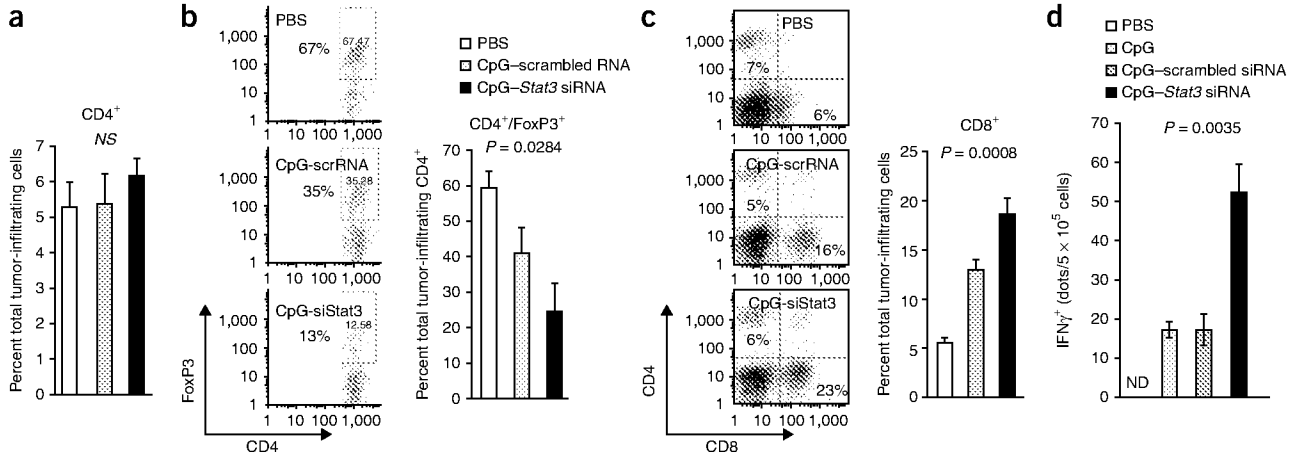

Figure 6 Targeting Stat3 using CpG–*Stat3* siRNA augments innate and adaptive antitumor immunity. Effects of *in vivo* CpG–*Stat3* siRNA treatment on immune cell populations within tumor. (**a**–**d**) Single-cell suspensions prepared from tumors pooled from three to six mice/group were analyzed by flow cytometry for the presence of CD4$^+$ (**a**), CD4$^+$FoxP3$^+$ (**b**) and CD8$^+$ (**c**). Representative dot plots (left panels in **b**,**c**) and means ± s.e.m. combining three independent experiments (right panels in **b**,**c**) are shown. NS, not significant. (**d**) Local treatments with CpG–*Stat3* siRNA generate tumor antigen–specific immune responses. IFNγ ELISPOT assays were performed using cell suspensions prepared from four pooled TDLNs per each treatment group; presented are the results from one of two independent experiments. Bars represent average numbers of TRP2-specific dots ± s.e.m. from triplicate samples. *P* values from one-way ANOVA test for statistical significance are indicated. ND, not detectable.

antigen-presenting cells. Fluorescent immunostaining of frozen tumor tissues with anti-CD8 antibody confirmed data generated by the flow cytometric analysis that CpG–*Stat3* siRNA treatment caused increased $CD8^+$ T-cell infiltration in tumors (data not shown). Activation of tumor antigen–specific $CD8^+$ T cells is believed to be critical for immune-mediated antitumor effects. We therefore examined the ability of CpG–*Stat3* siRNA treatment to generate $CD8^+$ T cells specific for the B16 tumor antigen, TRP2. Enzyme-linked immunosorbent spot (ELISPOT) assays to determine interferon (IFN)γ production by T cells isolated from TDLNs in response to recall stimulation with TRP2 peptide antigen indicated that *in vivo* CpG–*Stat3* siRNA administration indeed induced antigen-specific $CD8^+$ T cells (**Fig. 6d**).

DISCUSSION

We have developed a strategy that combines targeted siRNA delivery and activation of immune cells by covalently linking TLR oligonucleotide agonists to siRNAs. These conjugates encompass three activities in a single molecule: immune cell targeting, TLR activation and immune checkpoint silencing. In addition to TLR9, which was targeted in this study, several other intracellular TLRs, such as TLR3, TLR7 and TLR8, also interact with nucleic acids, suggesting a broad applicability of this approach. Different immune cells could be targeted by using various ligands for these TLRs. TLRs are important for stimulating DC maturation, antigen uptake and presentation, leading to cytotoxic T-lymphocyte activation and $CD4^+$ T helper cell differentiation. Therefore, TLR agonist–siRNA approaches can further stimulate desired immune responses for treating diseases such as cancer and infections. Although it has been established that binding to TLR9 is necessary for CpG-mediated immune activation, it remains to be fully explored how CpG oligonucleotides enter cells[36]. Our results indicated that cellular uptake of both CpG oligonucleotide and the CpG-siRNA constructs can occur in the absence of TLR9. However, TLR9, at least in mouse cells, is essential for CpG-siRNA–mediated gene silencing. Although the exact underlying mechanism(s) remains to be determined, it is possible that triggering TLR9 could effect either endosomal release of CpG-siRNA into the cytoplasm, and/or its intracellular processing.

Although TLR9 is expressed in different types of mouse DCs, its expression is more selective in humans. Whereas the highest levels of constitutive TLR9 expression is observed on human plasmacytoid DCs and B cells, it is also expressed at lower levels on human monocytes and macrophages[26]. These immune cells can serve as antigen-presenting cells and induce innate, adaptive or humoral immunity[27,29,46]. A critical role of tumor stromal macrophages and B cells in promoting tumor development has been well documented[47,48]. Importantly, Stat3 and several other molecules produced by the tumor myeloid population, and possibly tumor-associated B cells, are critical for tumor immunosuppression[17], and Stat3 activity in the myeloid compartment (and possibly in B cells as well) promotes Stat3 activity in tumor cells and endothelial cells in the tumor, enhancing tumor cell growth and/or survival[12,21–23]. In addition to Stat3, other oncogenic molecules produced by the tumor myeloid/B-cell compartment are also critical in promoting cancer growth and resistance to various therapies. Therefore, being able to target the tumor stromal myeloid cells and/or B cells through CpG-siRNA conjugate molecules is highly desirable for cancer therapies. In addition to normal immune cells, several types of tumor cells, including those of B-cell origin, and some solid tumor cells, are also positive for TLR9 (ref. 49). Our preliminary results suggested the feasibility of the CpG-siRNA approach to silence genes in $TLR9^+$ tumor cells. For example, treating human $TLR9^+$ tumors in nonobese diabetic/severe combined immunodeficient/*IL-2Rγ* knockout mice with CpG–*Stat3* siRNA resulted in tumor cell apoptosis and tumor growth inhibition (M. Kortylewski and H.Y., unpublished data). More experiments remain to be performed to optimize this approach for potential clinical use.

Our results indicated that the gene silencing effects by CpG-siRNA in cultured cells require high concentrations of the conjugates relative to those required *in vivo*. Work is underway to determine the possible cause(s) of this difference, which might include serum-associated degradation of CpG-siRNAs or reduction of the overall silencing effect in rapidly dividing cell populations. It is possible that repeated treatments *in vivo* allow accumulative gene silencing effects, and the crosstalk between various cells in the tumor microenvironment could lead to secondary inhibitory effects on Stat3 activity[23]. The half-life of the constructs at present is limited. Although the CpG oligonucleotide in the construct is phosphothioated, which should resist serum degradation, the siRNA in the chimeric construct is unmodified and negatively charged. Chemically modifying the siRNA to prolong serum stability and to neutralize the negative charge of the siRNA to facilitate endosomal release may improve the efficacy of the TLR agonist–siRNA approach. Furthermore, it has been demonstrated recently that adding triphosphate to the 5′ of siRNA can potentiate the antitumor effects of siRNA by stimulating antitumor immune responses, likely through intracellular RNA sensors such as RIG-I or MDA-5 (ref. 4). It is therefore conceivable that the triphosphate can be incorporated into the CpG-siRNA to further amplify antitumor immunity.

Although more studies are necessary to further understand the mechanism(s), and to improve CpG-siRNA gene silencing effects, our results raise the possibility of using oligonucleotide TLR agonists for siRNA delivery into tumor-associated myeloid cells and B cells, and possibly to certain tumor cells, to inhibit expression of tumor-promoting/immunosuppressive molecules while activating TLR(s) for immune activation.

METHODS

Methods and any associated references are available in the online version of the paper at http://www.nature.com/naturebiotechnology/.

Note: Supplementary information is available on the Nature Biotechnology website.

ACKNOWLEDGMENTS

We are grateful to the Light Microscopy Imaging and Flow Cytometry Cores and Animal Facilities of Beckman Research Institute at City of Hope Medical Center for technical support and assistance and X. Li of the Department of Biomedical Informatics for consultation on statistical analyses. We thank C.H. Contag of Stanford University School of Medicine for providing the original luciferase mice. Mouse dendritic DC2.4 cells were originally from K. Rock (University of Massachusetts Medical School). The highly metastatic clone of K1735 melanoma (C4) was kindly provided by S. Huang and J. Fidler of M.D. Anderson Cancer Center. The stably transduced A20-Luc cell line was provided by D. Zheng (City of Hope). This work is funded in part by grants from the board of governors for City of Hope Medical Center, Harry Lloyd Charitable Trust and Keck Foundation, in addition to National Institutes of Health grants (R01CA122976, R01CA115815, R01CA115674, P50CA107399).

AUTHOR CONTRIBUTIONS

H.Y. and M. Kortylewski conceived the project, designed the majority of the experiments, analyzed the data and wrote the paper. M. Kortylewski also carried out many of the key experiments and was instrumental in the design of the CpG-siRNA construct. P.S. contributed to the design of the construct and synthesized all the CpG-siRNA constructs. A.H. performed imaging and EMSA experiments. L.W. did A20 tumor cell experiments and luciferase CpG-siRNA experiments *in vivo*. C.K. tested siRNA sequences and carried out all the real-time PCR experiments. M. Kujawski and Y.L. performed some *in vivo* experiments. H.L. and C.Y. did western blot analysis. A.S. and J.D. tested CpG-siRNA in B-cell malignant cells. H.S.S. suggested the *in vitro* Dicer experiment. A.R. contributed to the MC38-CEA tumor experiment. J.J.R. and S.F. provided helpful discussion. J.J.R. was also

© 2009 Nature America, Inc. All rights reserved.

helpful in the siRNA design. D.M.P. contributed to immunological experimental design, provided insightful discussion and assisted in writing the manuscript. R.J. contributed to the concept of the project and the Stat3 siRNA design.

Published online at http://www.nature.com/naturebiotechnology/.
Reprints and permissions information is available online at http://npg.nature.com/reprintsandpermissions/.

1. Song, E. *et al.* Antibody mediated *in vivo* delivery of small interfering RNAs via cell-surface receptors. *Nat. Biotechnol.* **23**, 709–717 (2005).
2. McNamara, J.O. II *et al.* Cell type-specific delivery of siRNAs with aptamer-siRNA chimeras. *Nat. Biotechnol.* **24**, 1005–1015 (2006).
3. Kumar, P. *et al.* Transvascular delivery of small interfering RNA to the central nervous system. *Nature* **448**, 39–43 (2007).
4. Poeck, H. *et al.* 5′-Triphosphate-siRNA: turning gene silencing and Rig-I activation against melanoma. *Nat. Med.* **14**, 1256–1263 (2008).
5. Li, B.J. *et al.* Using siRNA in prophylactic and therapeutic regimens against SARS coronavirus in Rhesus macaque. *Nat. Med.* **11**, 944–951 (2005).
6. Zimmermann, T.S. *et al.* RNAi-mediated gene silencing in non-human primates. *Nature* **441**, 111–114 (2006).
7. Bui, J.D. & Schreiber, R.D. Cancer immunosurveillance, immunoediting and inflammation: independent or interdependent processes? *Curr. Opin. Immunol.* **19**, 203–208 (2007).
8. Koebel, C.M. *et al.* Adaptive immunity maintains occult cancer in an equilibrium state. *Nature* **450**, 903–907 (2007).
9. Shankaran, V. *et al.* IFNgamma and lymphocytes prevent primary tumour development and shape tumour immunogenicity. *Nature* **410**, 1107–1111 (2001).
10. Kortylewski, M. *et al.* Inhibiting Stat3 signaling in the hematopoietic system elicits multicomponent antitumor immunity. *Nat. Med.* **11**, 1314–1321 (2005).
11. Zou, W. Immunosuppressive networks in the tumour environment and their therapeutic relevance. *Nat. Rev. Cancer* **5**, 263–274 (2005).
12. Kujawski, M. *et al.* Stat3 mediates myeloid cell-dependent tumor angiogenesis in mice. *J. Clin. Invest.* **118**, 3367–3377 (2008).
13. Yu, C.L. *et al.* Enhanced DNA-binding activity of a Stat3-related protein in cells transformed by the Src oncoprotein. *Science* **269**, 81–83 (1995).
14. Bromberg, J.F. *et al.* Stat3 as an oncogene. *Cell* **98**, 295–303 (1999).
15. Yu, H. & Jove, R. The STATs of cancer–new molecular targets come of age. *Nat. Rev. Cancer* **4**, 97–105 (2004).
16. Darnell, J.E. Jr. Transcription factors as targets for cancer therapy. *Nat. Rev. Cancer* **2**, 740–749 (2002).
17. Yu, H., Kortylewski, M. & Pardoll, D. Crosstalk between cancer and immune cells: role of STAT3 in the tumour microenvironment. *Nat. Rev. Immunol.* **7**, 41–51 (2007).
18. Wang, T. *et al.* Regulation of the innate and adaptive immune responses by Stat-3 signaling in tumor cells. *Nat. Med.* **10**, 48–54 (2004).
19. Kortylewski, M. & Yu, H. Role of Stat3 in suppressing anti-tumor immunity. *Curr. Opin. Immunol.* **20**, 228–233 (2008).
20. Kortylewski, M. *et al.* Regulation of the IL-23 and IL-12 balance by Stat3 signaling in the tumor microenvironment. *Cancer Cell* **15**, 114–123 (2009).
21. Bollrath, J. *et al.* gp130-mediated Stat3 activation in enterocytes regulates cell survival and cell-cycle progression during colitis-associated tumorigenesis. *Cancer Cell* **15**, 91–102 (2009).
22. Grivennikov, S. *et al.* IL-6 and Stat3 are required for survival of intestinal epithelial cells and development of colitis-associated cancer. *Cancer Cell* **15**, 103–113 (2009).
23. Lee, H. *et al.* Persistently activated Stat3 maintains constitutive NF-kappaB activity in tumors. *Cancer Cell* **15**, 283–293 (2009).
24. Wang, L. *et al.* IL-17 is pro-carcinogenic through an IL-6/Stat3 signaling pathway. *J. Exp. Med.* **206**, 1457–1464 (2009).
25. Kortylewski, M. *et al.* Toll-like receptor 9 activation of signal transducer and activator of transcription 3 constrains its agonist-based immunotherapy. *Cancer Res.* **69**, 2497–2505 (2009).
26. Iwasaki, A. & Medzhitov, R. Toll-like receptor control of the adaptive immune responses. *Nat. Immunol.* **5**, 987–995 (2004).
27. Kanzler, H., Barrat, F.J., Hessel, E.M. & Coffman, R.L. Therapeutic targeting of innate immunity with Toll-like receptor agonists and antagonists. *Nat. Med.* **13**, 552–559 (2007).
28. Barchet, W., Wimmenauer, V., Schlee, M. & Hartmann, G. Accessing the therapeutic potential of immunostimulatory nucleic acids. *Curr. Opin. Immunol.* **20**, 389–395 (2008).
29. Krieg, A.M. Toll-like receptor 9 (TLR9) agonists in the treatment of cancer. *Oncogene* **27**, 161–167 (2008).
30. Klinman, D.M., Currie, D., Gursel, I. & Verthelyi, D. Use of CpG oligodeoxynucleotides as immune adjuvants. *Immunol. Rev.* **199**, 201–216 (2004).
31. Klinman, D.M., Yi, A.K., Beaucage, S.L., Conover, J. & Krieg, A.M. CpG motifs present in bacteria DNA rapidly induce lymphocytes to secrete interleukin 6, interleukin 12, and interferon gamma. *Proc. Natl. Acad. Sci. USA* **93**, 2879–2883 (1996).
32. Krieg, A.M. *et al.* CpG motifs in bacterial DNA trigger direct B-cell activation. *Nature* **374**, 546–549 (1995).
33. Kim, D.H. *et al.* Synthetic dsRNA Dicer substrates enhance RNAi potency and efficacy. *Nat. Biotechnol.* **23**, 222–226 (2005).
34. Rose, S.D. *et al.* Functional polarity is introduced by Dicer processing of short substrate RNAs. *Nucleic Acids Res.* **33**, 4140–4156 (2005).
35. Hemmi, H. *et al.* Toll-like receptor recognizes bacterial DNA. *Nature* **408**, 740–745 (2000).
36. Latz, E. *et al.* TLR9 signals after translocating from the ER to CpG DNA in the lysosome. *Nat. Immunol.* **5**, 190–198 (2004).
37. Chendrimada, T.P. *et al.* TRBP recruits the Dicer complex to Ago2 for microRNA processing and gene silencing. *Nature* **436**, 740–744 (2005).
38. Samarasinghe, R. *et al.* Induction of an anti-inflammatory cytokine, IL-10, in dendritic cells after toll-like receptor signaling. *J. Interferon Cytokine Res.* **26**, 893–900 (2006).
39. Cao, Y.A. *et al.* Shifting foci of hematopoiesis during reconstitution from single stem cells. *Proc. Natl. Acad. Sci. USA* **101**, 221–226 (2004).
40. Benkhart, E.M., Siedlar, M., Wedel, A., Werner, T. & Ziegler-Heitbrock, H.W. Role of Stat3 in lipopolysaccharide-induced IL-10 gene expression. *J. Immunol.* **165**, 1612–1617 (2000).
41. Xie, T.X. *et al.* Stat3 activation regulates the expression of matrix metalloproteinase-2 and tumor invasion and metastasis. *Oncogene* **23**, 3550–3560 (2004).
42. Takeda, K. *et al.* Enhanced Th1 activity and development of chronic enterocolitis in mice devoid of Stat3 in macrophages and neutrophils. *Immunity* **10**, 39–49 (1999).
43. Welte, T. *et al.* STAT3 deletion during hematopoiesis causes Crohn's disease-like pathogenesis and lethality: a critical role of STAT3 in innate immunity. *Proc. Natl. Acad. Sci. USA* **100**, 1879–1884 (2003).
44. Dhodapkar, M.V., Steinman, R.M., Krasovsky, J., Munz, C. & Bhardwaj, N. Antigen-specific inhibition of effector T cell function in humans after injection of immature dendritic cells. *J. Exp. Med.* **193**, 233–238 (2001).
45. Bui, J.D., Uppaluri, R., Hsieh, C.S. & Schreiber, R.D. Comparative analysis of regulatory and effector T cells in progressively growing versus rejecting tumors of similar origins. *Cancer Res.* **66**, 7301–7309 (2006).
46. Klinman, D., Shirota, H., Tross, D., Sato, T. & Klaschik, S. Synthetic oligonucleotides as modulators of inflammation. *J. Leukoc. Biol.* **84**, 958–964 (2008).
47. Sica, A. & Bronte, V. Altered macrophage differentiation and immune dysfunction in tumor development. *J. Clin. Invest.* **117**, 1155–1166 (2007).
48. Tan, T.T. & Coussens, L.M. Humoral immunity, inflammation and cancer. *Curr. Opin. Immunol.* **19**, 209–216 (2007).
49. Spaner, D.E., Foley, R., Galipeau, J. & Bramson, J. Obstacles to effective Toll-like receptor agonist therapy for hematologic malignancies. *Oncogene* **27**, 208–217 (2008).

© 2009 Nature America, Inc. All rights reserved.

ONLINE METHODS

Cells. Murine B16 melanoma, CT26 colon carcinoma and A20 B cell lymphoma lines were purchased from American Type Culture Collection. Mouse dendritic DC2.4 cells were originally from K. Rock. Highly metastatic clone of K1735 melanoma (C4) was kindly provided by S. Huang and J. Fidler. The stably transduced A20-Luc cell line was provided by D. Zheng. The generation of transgenic C57BL/6.CEA mice and MC-38.CEA cell line was previously described[50].

Oligonucleotide design and synthesis. The phosphothioated oligodeoxyribonucleotide (oligonucleotide) and antisense strands (AS) of siRNAs were linked using 6 units of C3 carbon chain linker $(CH_2)_3$ (Glen Research). The resulting constructs were hybridized with complementary sense strands (SS) of siRNAs to create chimeric oligonucleotide-siRNA constructs used in the study (deoxynucleotides are shown underlined). Sequences of single-stranded constructs are listed below; the target *Stat3* sequence is found between bases 1898 and 1922 of the mouse *Stat3* gene (accession number NM_213659).

Mouse Stat3 siRNA (SS) 5′ CAGGGUGUCAGAUCACAUGGGCUAA 3′

CpG1668-mouse Stat3 siRNA(AS) 5′ TCCATGACGTTCCTGATGCT-linker-UUAGCCCAUGUGAUCUGACACCCUGAA 3′

GpC-mouse Stat3 siRNA (AS)

5′ TCCATGAGCTTCCTGATGCT-linker-UUAGCCCAUGUGAUCUGAC ACCCUGAA 3′

Scrambled RNA (SS)

5′ UCCAAGUAGAUUCGACGGCGAAGTG 3′

CpG1668–scrambled RNA (AS)

5′ TCCATGACGTTCCTGATGCT-linker-CACUUCGCCGUCGAAUCUA CUUGGAUU 3′

The sequence of firefly *luciferase*-specific 25-27-mer siRNA (Luc1 R 25D/27), used for the CpG1668-*Luc* siRNA conjugate molecule, was published[34]. The correct formation of siRNA duplex was confirmed by *in vitro* Dicer cleavage assays. 0.5 μg of each oligonucleotide-siRNA construct was subjected to processing by 1U of Dicer (Ambion) in 37 °C for 1.5 h, resolved with 15% polyacrylamide/7.5M urea gel and results of the dicing reaction were visualized with SYBR Gold staining (Invitrogen).

Quantitative real-time PCR. Total RNA was extracted from cultured or primary cells using RNeasy kit (Qiagen). After cDNA synthesis using iScript cDNA Synthesis kit (Bio-Rad), samples were analyzed using pairs of primers specific for *Stat3*, *TNF*, *IL-6*, *IP-10*, *RANTES*, *p35/IL-12*, *p40/IL-12* and *GAPDH* mRNAs (SuperArray Bioscience). Sequence-specific amplification was detected by fluorescent signal of SYBR Green (Bio-Rad) by using Chromo4 Real-time PCR Detector (Bio-Rad).

Transient transfections. B16 cells were transiently transfected with 15 nM CpG-linked or uncoupled *Stat3* siRNA and scrambled RNA using Lipofectamine 2000 (Invitrogen). 48 h later cells were lysed and used for western blot analysis.

EMSA and western blot analysis. EMSA and western blot analysis to detect Stat3 DNA-binding and protein expression were performed as described previously[18]. The protein levels of Stat3 detected by western blotting were later quantified by densitometry using AlphaEase FC software (Alpha Innotech).

Luciferase reporter gene assay. A20-Luc cells incubated with CpG-RNAs for 48 h or primary cells isolated from TDLNs of *Luc*$^+$ mice treated with CpG-*Luc* siRNA were lysed and luciferase activities were determined using the Luciferase Assay System (Promega) after normalization to the protein content of the sample.

***In vivo* experiments.** Mouse care and experimental procedures were performed under pathogen-free conditions in accordance with established institutional guidance and approved protocols from Research Animal Care Committees of the City of Hope. For s.c. tumor challenge, we injected 1×10^5 B16, MC38.CEA, C4 or CT26 tumor cells into 7–8 week-old C57BL/6, C57BL/6.CEA, C3H or Balb/C mice, respectively. After tumors reached average size of ~5 mm, mice were injected peritumorally with 0.78 nmol of CpG1668 oligonucleotide alone, in combination with *Stat3* siRNA or CpG/GpC oligonucleotide linked to various double-stranded RNA (dsRNA) sequences described above. Tumor growth was monitored every other day. For the analysis of cellular and molecular mechanisms of CpG/GpC-dsRNAs effects, mice were killed after 2–3 weeks of treatment. For experiments on silencing of luciferase activity *in vivo*, *Luc*$^+$ mice (originally kindly provided by C.H. Contag) were challenged with tumor and treated with three daily injections of CpG-*Luc* siRNA or CpG–scrambled RNA. Lymph nodes as well as tumor specimens were harvested. For B16 lung metastasis model, mice were challenged with 0.5×10^5 B16 tumor cells (i.v. injection) and 2 d later, after tumors were established, were treated systemically with 0.78 nmol (~1 mg/kg) of CpG1668 oligonucleotide or various CpG-dsRNAs. Intravenous injections were repeated every other day for 2 weeks. Lungs were harvested, fixed and the number of B16 tumor colonies was manually counted. The level of *Stat3* silencing was assessed by real-time PCR in DCs isolated from tumor-draining inguinal (for s.c. tumor model) or cervical (for metastasis model) lymph nodes. For immune cell depletion, mice were pretreated with anti-CD8 plus anti-CD4 antibodies (clone 2.43 and GK1.5, respectively, depleting 99% and 98% of CD8 and CD4 cells, respectively) or anti-asialo-GM1 antibodies (Wako, depleting min. 79% of NK cells) before tumor inoculation then injected weekly.

Flow cytometry and ELISA. We prepared single-cell suspensions of spleen, lymph node or tumor tissues by mechanic dispersion followed by collagenase D/DNase I treatment, as described[10]. For extracellular staining of immune markers, 1×10^6 of freshly prepared cells suspended in PBS/2% FCS/0.1% wt/vol sodium azide was preincubated with FcγIII/IIR-specific antibody to block nonspecific binding and stained with different combinations of fluorochrome-coupled antibodies to CD11c, I-A^b (MHCII), CD40, CD80, B220, CD11b, Gr1, CD3, CD8 or CD4 (BD Biosciences). Before intracellular staining with antibodies to TLR9 (eBioscience), Dicer (Santa Cruz) or FoxP3 (eBioscience), various immune cell subsets were fixed in paraformaldehyde and permeated in methanol. Fluorescence data were collected on FACScalibur (Beckton Dickinson) and analyzed using FlowJo software (Tree Star).

ELISPOT assay. 5×10^5 cells isolated form TDLNs of CpG- or CpG-siRNA–treated mice, were seeded into each well of 96-well filtration plate in the presence or absence of 10 μg/ml of TRP2 peptide. After 24 h of incubation at 37 °C, peptide-specific IFNγ-positive spots were detected according to manufacturer's procedure (Mouse IFNGγ ELISPOT, Cell Sciences), scanned and quantified using Immunospot Analyzer from Cellular Technology.

Fluorescent, confocal and intravital two-photon microscopy. For immunofluorescent staining, we fixed the flash-frozen tumor specimens in formaldehyde and permeabilized with methanol before antibody staining. For confocal microscopy, cultured cells were fixed with 2% paraformaldehyde for 20 min, permeabilized in PBS/0.1% Triton X-100/1 mM $MgCl_2$, and 0.1 mM $CaCl_2$ for 5 m and quenched in 50 mM NH_4Cl for 5 min before blocking in 1% BSA for 1 h. Samples were stained with antibodies to CD11b (BD Biosciences), neutrophils (7/4, Cedarlane), active caspase-3 (Cell Signaling), TLR9, Dicer and detected with Alexa488- or Alexa555-coupled secondary antibodies (Invitrogen). After staining the nuclei with DAPI (Vector) or Hoechst 33342, slides were mounted and analyzed by fluorescent or confocal microscopy. The confocal imaging was carried out using a 63× water immersion objective on cLSM510Meta confocal microscope (Zeiss). For intravital two-photon imaging, B16 tumor-bearing mice received single intratumoral injection of 0.78 nmol FITC-labeled CpG–*Stat3* siRNA, followed by retro-orbital injection of dextran-rhodamine (Invitrogen) and Hoechst 33342 before imaging 1 h later. Mice were anesthetized and intravital two-photon microscopy was carried out using equipment and software from Ultima Multiphoton Microscopy Systems.

Statistical analysis. Unpaired *t*-test with equal or unequal variance (specifically for the analysis of cytokine expression in **Fig. 5a**) was used to calculate two-tailed *P* value to estimate statistical significance of differences between two treatment groups in the whole study. One-way ANOVA followed by Newman-Keuls test was applied for comparison of multiple-treatment groups. Two-way ANOVA plus Bonferroni post-test were applied to assess statistical significance of differences in tumor growth kinetics between multiple treatment groups. Statistically significant *P* values were indicated in figures and/or legends. ***, $P < 0.001$; **, $P < 0.01$; *, $P < 0.05$. Data were analyzed using GraphPad Prism version 4.0 software (GraphPad).

50. Clarke, P., Mann, J., Simpson, J.F., Rickard-Dickson, K. & Primus, F.J. Mice transgenic for human carcinoembryonic antigen as a model for immunotherapy. *Cancer Res.* **58**, 1469–1477 (1998).

© 2009 Nature America, Inc. All rights reserved.